A scattering spectroscopy of a superconducting artificial atom, coupled to two half spaces

A.Yu.Dmitriev,[1,*] A.Korenkov,[2,1] and O.V.Astafiev[3,1,4]

[1] *Moscow Institute of Physics and Technology, 141700 Dolgoprudny, Russia*
[2] *Skolkovo Institute of Science and Technology, 143026 Moscow, Russia*
[3] *Physics Department, Royal Holloway, University of London, Egham, Surrey TW20 0EX, United Kingdom*
[4] *Russian Quantum Center, 100 Novaya Street, Skolkovo, Moscow region 143025, Russia.*

(Dated: December 2, 2016)

We propose a novel approach for spectroscopic characterization of quantum systems. A superconducting quantum system — an artificial atom — is coupled asymmetrically to two open-end transmission lines (1D half-spaces). The lines themselves are strongly decoupled from each other. This results in suppression of the direct microwave propagation from one side to another. The atom, excited from the weaker coupled side relaxes with photon emission preferably to the stronger coupled side. By measuring the emission spectrum we reconstruct the energy levels of the artificial atom. Our method allows to reject the excitation tone and to detect only the elastically scattered emission corresponding to interatomic transitions. We also demonstrate visualization of the higher-level transitions by populating the excited levels. Such a system does not have an optical analog with natural atoms or quantum dots coupled to two half spaces.

Introduction. The superconducting quantum system – an electrical circuit on a chip with quantized energy levels – is now commonly called artificial atoms. The atomic spectra, defined by the nano-scale circuit and controlled by external fields typically lay in the microwave (MW) frequency range. The atoms can be coupled to other circuit elements, such as other quantum systems, resonators, etc, and a physically strong coupling regime could be easily achieved [1]. This was successfully used to demonstrate exciting physics in the new field of on-chip quantum optics [2–5]. In an alternative approach, the artificial atoms could be directly plugged into a coplanar waveguide. This has been demonstrated to reach nearly 100% of scattering of propagating waves [6]. This regime of *microwave quantum optics* [7] suggests several very promising applications in quantum information processing and development of novel on-chip quantum electronics, utilising quantum properties of light.

In this work we realise a method of spectroscopy of artificial atoms (with several lowest levels) asymmetrically coupled to a pair of open-end transmission lines on a chip, working as two 1D half-spaces. Physically the on-chip circuit is similar to the one realized in [8]: the atom can be driven via a weakly coupled input line, however the driving wave is largely reflected back due to mismatch of impedances. The resonant to the atomic transition light is partially absorbed by artificial atom resulting in the atomic excitation. Then the atom relaxes with the photon emission into the output (emission) line. The radiation is then amplified and detected. Importantly, only resonantly scattered light is emitted to the output line and, therefore detected. The spectrum of detected light visualises atomic transitions.

In order to efficiently detect the light we use a network analyser (NT) sensing only coherently emitted radiation at the excitation frequency due to an atomic dipole emission. In order to detect higher level transitions, we apply a technique of population of the lower levels. This is achieved by adding another tone resonant with lower transitions, e.g. $|0\rangle \leftrightarrow |1\rangle$ populates state $|1\rangle$. As a result of the population, the spectral line corresponding to $|1\rangle \leftrightarrow |2\rangle$ transition can be observed. Our N-level system

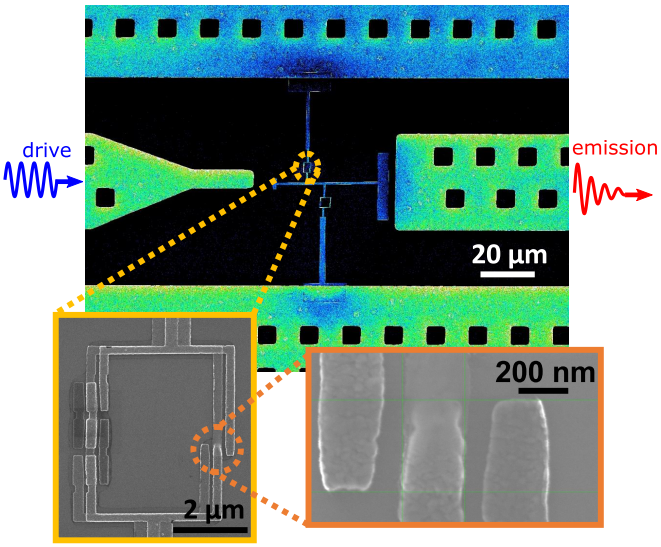

FIG. 1. Sample SEM image. An upper panel shows the general layout of the transmission lines and the artificial atom. The left line, weaker coupled to the loop (see enlarged view on the bottom left panel) is the input line, from which the driving field is applied. The right-hand side line is the output (emission) line stronger coupled to the atom. The atom is designed as flux qubit with four Josephson junctions.

driven by the external fields is approximated as

$$H = \sum_{j}^{N} \hbar\omega_j |j\rangle\langle j| - \hbar\Omega_{jl}(|j\rangle\langle l| + |l\rangle\langle j|)\cos\omega_{jk}t, \quad (1)$$

where $|j\rangle\langle l|$ are projection operators of our system, driven by the classical MW fields with frequency ω_{jl} and amplitudes Ω_{jl}. The coherent waves emitted into the output line are

$$V_{jl} = -\frac{\hbar\Gamma_1^{jl}}{\mu}\langle|j\rangle\langle l|\rangle e^{i\omega_{jl}t-ikx}, \quad (2)$$

where μ is the dipole moment of the atom, Γ_1^{jl} is the radiative emission rate at frequency ω_{jl} and k is the wavevector of the emitted wave. The emission line is as narrow as the drive, which is hardware-defined by a linewidth of the MW generator and has an order of several Hz. Such a narrow spectrum allows to measure the amplified signal by the linear detectors (NTs) with a very narrow bandwidth and therefore reduce the signal-to-noise ratio.

The device. Our device has a geometry of a 4-junction flux qubit [6, 9] fabricated on a silicon substrate by a standard technique of two-angle shadow deposition, see Fig. 1. Three junctions have areas of $0.2 \times 0.8\ \mu m$, and one is $\alpha \approx 0.35$ (area ratio) times smaller. One side of the α-junction is effectively grounded and another one is coupled the transmission lines. An input line is coupled to the atom via small capacitance $C_i \approx 0.5$ fF, and a larger one $C_e \approx 2.8$ fF couples the atom to the output (emission) line so that the total effective α-junction capacitance is a sum of the junction capacitance itself $C_\alpha \approx 2.5$ fF and the both coupling capacitances $(C_\alpha + C_i + C_e)$. The persistent current, $I_p = 18$ nA, in the loop is lower, comparing to standard flux qubits, due to low Josephson energies, which makes the system less sensitive to the flux noise. This could result in significantly increased dephasing times, up to tens of microseconds [10] but reduces the anharmonicity similar to transmon qubits [11]. For our samples, the anharmonicity of about 1.5 GHz is still large enough for two-level approximation valid even for high driving powers. At the same time, the higher levels $|2\rangle$ and $|3\rangle$ are shifted down in energies, so that frequencies of higher transitions $|1\rangle \leftrightarrow |2\rangle$ and $|2\rangle \leftrightarrow |3\rangle$ are within the range of HEMT amplifier (1-12 GHz) and the transition frequencies could be probed directly by linear detectors.

The experiment. To probe our atom, we place it within a specially designed sample holder, with MW coplanar lines. The holder is mounted to the lowest stage of the Bluefors-LD250 dilution refrigerator and is cooled down to a temperature of 15 mK. At that temperature $k_B T \ll \hbar\omega_{01}$ and the atom in rest is in well defined ground state $|0\rangle$. The strong coupling regime between the atom and the output transmission line is realised if the non-radiative decay rate $\Gamma_{\rm NR}$ of state $|1\rangle$ is much smaller than the natural linewidth Γ_1^{01} due to spontaneous emission into the output line. In case of a single atom plugged into a continuos coplanar transmission line [6, 12] this is manifested in nearly full reflection of a weak MW with the frequency ω close to $\omega_{01} = (E_1 - E_0)/\hbar$: Reflection coefficient r can reach unity if $\omega = \omega_{01}$, while far away from resonance $r = 0$. It means that the light is fully scattered on a single quantum system. In our scheme with asymmetric coupling to two separated half-spaces, the resonant drive applied from the input line excites the atom. The radiative relaxation could result in the emission to either line but as it was shown in [8], the power is emitted to the output line with efficiency $1 - C_i^2/C_e^2 \approx 0.97$ and, in principle, by optimising the capacitances could be made arbitrary close to one. Note that the same system can operate as a single microwave photon source, when π-pulse is applied.

In our experiment, we exploit another useful feature of this system based on elastic scattering of the coherent radiation. The input and output lines are decoupled from each other due to impedance mismatch: $Z_s = 1/j\omega_{01}C_i \approx 6 \cdot 10^4\ \Omega$ is much larger than line impedance $Z_0 = 50\ \Omega$, and almost all power applied to the input line is reflected back. Therefore the states of light in output mode is nothing more but quantum light emitted by the atom. Consequently, monitoring the spectrum and/or intensity of coherent output waves, one can acquire important information about energies of the artificial atom. To study the spectrum we use a network analyser and detect the amplitude and phase of the coherent radiation emitted by the atom at the excitation frequency ω.

We begin with probing the lowest transition between levels $|0\rangle$ and $|1\rangle$ by applying a MW signal to the input line at frequency ω swept in a wide range, and measuring the output emission. The input signal excites the atom only if ω is close to ω_{01}. Figure 2a demonstrates typical spectrum obtained by the NT as a function of frequency and an external flux bias Φ. Note that the corresponding single-photon power $P_{01} = \hbar\Gamma_1^{01}\omega_{01}\langle|0\rangle\langle 1|\rangle$ is limited by relaxation rate Γ_1^{01}: the atom can not emit more than a single photon at a time. Therefore, in this measurement the power of input signal effectively seen by qubit must be $P \sim P_{01} \sim 10^{-17}$ Watt. The bright line at the density plot corresponds to the transition ω_{01}. Here, only lowest transition can be observed. Others (e.g. $|1\rangle \leftrightarrow |2\rangle$) are not visible because the unpopulated atom does not scatter the waves.

Now, we demonstrate the method of measuring the $|1\rangle \leftrightarrow |2\rangle$ transition. To do that we irradiate the atom by an additional tone at the ω_{01}, determined from the previous set of measurements, with the power increased up to $\sim 10^{-13}$ Watt. Another probe tone is of low power $\sim P_{01}$, with a frequency swept in the same range as in Fig. 2a. The first tone results in saturation of the atomic

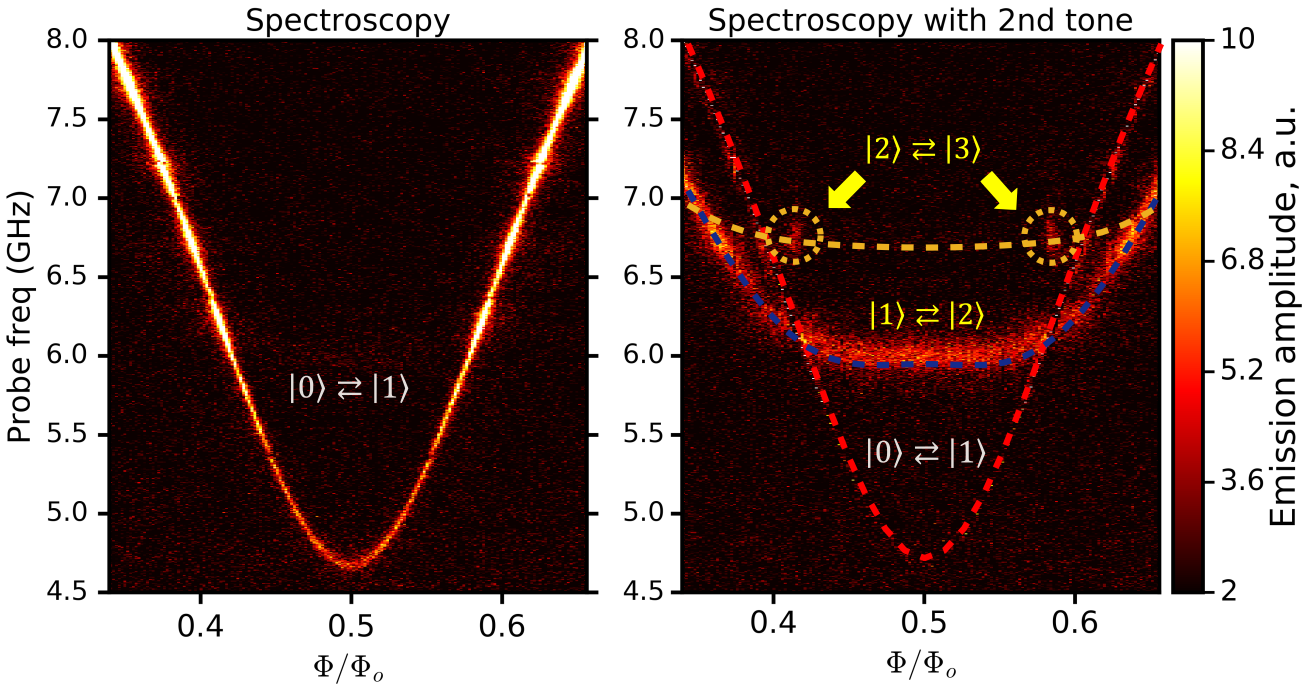

FIG. 2. Spectroscopy. The emission amplitudes measured by a network analyser as a function of frequency and flux bias Φ. (a) Directly measured $|0\rangle \leftrightarrow |1\rangle$ transition. (b) The $|1\rangle \leftrightarrow |2\rangle$ transition, measured when the lower $|0\rangle \leftrightarrow |1\rangle$ transition (red dashed spectral line) is excited by applying an additional tone at ω_{01}. The dashed lines are the transition frequencies obtained from numerical fitting. In addition, if $\omega_{01} = \omega_{12}$ then the level $|2\rangle$ is copulated and the emission from and $|2\rangle \leftrightarrow |3\rangle$ transition is also observed (regions marked by dashed yellow circles)

population of $|0\rangle$ and $|1\rangle$ to approximately 50%. Then, the applied probe signal may now excite the atom from $|1\rangle$ to $|2\rangle$. And the atom can emit the coherent waves at frequencies close at the transition frequency $\omega_{12} = (E_2 - E_1)/h$. This is confirmed by the observation of the new spectral line in Fig.2b, which has not been observed in the previous measurement. In addition to the ω_{12} transition, there are two bright spots at $\Phi \approx 0.42\Phi_0$ and $\Phi \approx 0.58\Phi_0$ (where Φ_0 is the flux quantum) and $\omega/2\pi \approx 6.7$ GHz, which we attribute to higher transition $|2\rangle \leftrightarrow |3\rangle$.

By measuring the scattered radiation, we can extract the detailed atomic properties, for example, relaxation times. Figure 3 demonstrates the transmission coefficient amplitude at the degeneracy point ($\Phi = \Phi_0$). The transmission of $|0\rangle \leftrightarrow |1\rangle$ is shown as the blue peak and $|1\rangle \leftrightarrow |2\rangle$ transitions is the magenta peak in the inset. By fitting it to the Lorentzian

$$P(\omega) = \frac{1}{\pi} \frac{\Gamma/2}{(\omega - \omega_0)^2 + (\Gamma/2)^2}, \qquad (3)$$

we extract the values for relaxation rates $\Gamma_1^{01}/2\pi = 20.8$ MHz and $\Gamma_1^{12}/2\pi = 192.4$ MHz. This particularly results in the emission power from the lowest transmission $P_{01} \sim 10^{-17}$ Watt. As we have mentioned above, the transition rate between states $|m\rangle$ and $|n\rangle$ is defined by the radiative decay to the open output line and can be calculated if all the system parameters are known [2, 6].

To fit the energy spectra and estimate the parameters of the device, we make a numerical diagonalzation of the four-junction Hamiltonian in the charge basis. The resulting spectra of a system is presented by dashed lines in Fig. 2b and is in a very good agreement with the experimental data. Moreover, we derive also the frequency ω_{23} of $|2\rangle \leftrightarrow |3\rangle$ transition, shown by yellow dashed line in Fig. 2b.

At last we demonstrate how the effective transition between the excited states ($|1\rangle \leftrightarrow |2\rangle$) depends on the lower transition drive amplitude Ω_{01}. The transmission amplitude at $|1\rangle \leftrightarrow |2\rangle$ shown on Fig. 4 is measured as a function of Ω_{01}. The curve has a maximum at $\Omega_{01}/2\pi \approx 10$ MHz, when it is roughly equal to Γ_1^{01}. Overdrive results in the suppression of the transmission.

In conclusion, we have demonstrated a new way of artificial atom spectroscopy by separating the drive and emission waves using asymmetric coupling to a pair of open-end transmission lines. The coherent emission is detected from the output line. Using our technique, we derived a spectrum of a three-level system and relaxation times. The method will be useful for applications in quantum optics based on microwave quantum circuits.

Acknowledgements. We acknowledge Russian Science Foundation (grant No.16-12-00070).

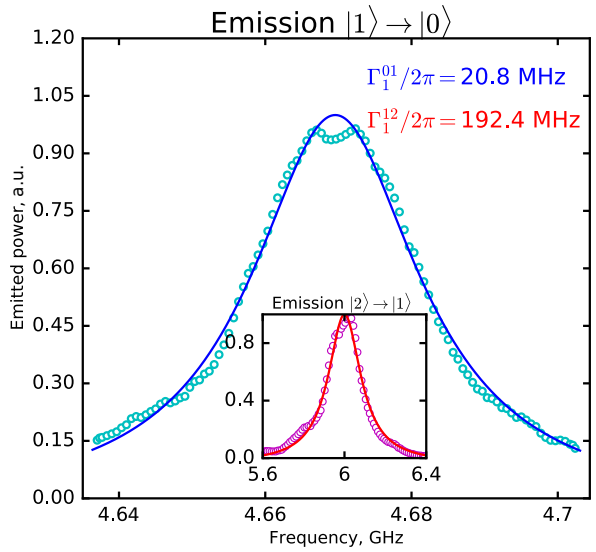

FIG. 3. An intensity of coherent emission. An artificial atom is irradiated by monochromatic driving signal, and the power of light elastically scattered by atom is measured. In case of small drive, the responce of $|i\rangle \leftrightarrow |j\rangle$ transition has Lorentzian shape [6] with the FWHM equal to Γ_1^{ij}.

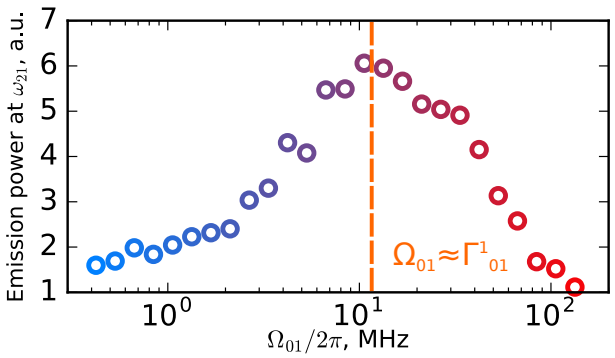

FIG. 4. The effect of $|0\rangle \leftrightarrow |1\rangle$ transition pumping amplitude on the $|1\rangle \leftrightarrow |2\rangle$ emission amplitude. The optimal pumping (the strongest emission) corresponds to the case when $\Omega_{01} \approx \Gamma_1^{01}$.

* dmitrmipt@gmail.com

[1] A. Wallraff, D. I. Schuster, A. Blais, L. Frunzio, R.-S. Huang, J. Majer, S. Kumar, S. M. Girvin, and R. J. Schoelkopf, Nature **431**, 162 (2004).

[2] O. V. Astafiev, A. A. Abdumalikov, A. M. Zagoskin, Y. A. Pashkin, Y. Nakamura, and J. S. Tsai, Phys. Rev. Lett. **104**, 183603 (2010).

[3] A. A. Abdumalikov Jr, O. V. Astafiev, Y. A. Pashkin, Y. Nakamura, and J. Tsai, Phys. Rev. Lett. **107**, 043604 (2011).

[4] A. A. Houck, D. I. Schuster, J. M. Gambetta, J. A. Schreier, B. R. Johnson, J. M. Chow, L. Frunzio, J. Majer, M. H. Devoret, S. M. Girvin, and R. J. Schoelkopf, Nature **449**, 328 (2007).

[5] M. Hofheinz, E. M. Weig, M. Ansmann, R. C. Bialczak, E. Lucero, M. Neeley, A. D. Oconnell, H. Wang, J. M. Martinis, and A. Cleland, Nature **454**, 310 (2008).

[6] O. Astafiev, A. M. Zagoskin, A. Abdumalikov, Y. A. Pashkin, T. Yamamoto, K. Inomata, Y. Nakamura, and J. Tsai, Science **327**, 840 (2010).

[7] J. Q. You and F. Nori, Nature **474**, 589 (2011).

[8] Z. Peng, S. de Graaf, J. Tsai, and O. Astafiev, Nature Communications **7**, 12588 (2016).

[9] Y. Qiu, W. Xiong, X.-L. He, T.-F. Li, and J. Q. You, Scientific Reports **6**, 28622 (2016).

[10] F. Yan, S. Gustavsson, A. Kamal, J. Birenbaum, A. P. Sears, D. Hover, T. J. Gudmundsen, D. Rosenberg, G. Samach, S. Weber, J. L. Yoder, T. P. Orlando, J. Clarke, A. J. Kerman, and W. D. Oliver, Nature Communications **7**, 12694 (2016).

[11] J. Koch, T. M. Yu, J. Gambetta, A. A. Houck, D. I. Schuster, J. Majer, A. Blais, M. H. Devoret, S. M. Girvin, and R. J. Schoelkopf, Phys. Rev. A **76**, 042319 (2007).

[12] I.-C. Hoi, C. Wilson, G. Johansson, J. Lindkvist, B. Peropadre, T. Palomaki, and P. Delsing, New Journal of Physics **15**, 025011 (2013).